Vol. 538: 35–52, 2015
doi: 10.3354/meps11385

MARINE ECOLOGY PROGRESS SERIES
Mar Ecol Prog Ser

Published October 28

# Community metabolism in shallow coral reef and seagrass ecosystems, lower Florida Keys

**D. Turk[1,2,*], K. K. Yates[3], M. Vega-Rodriguez[4], G. Toro-Farmer[4], C. L'Esperance[1], N. Melo[5,6], D. Ramsewak[7], M. Dowd[1], S. Cerdeira Estrada[8], F. E. Muller-Karger[4], S. R. Herwitz[9], W. R. McGillis[2]**

[1]Dalhousie University, Halifax, NS B3H 4R2, Canada
[2]LDEO, Columbia University, New York, NY 10964, USA
[3]U.S. Geological Survey, St. Petersburg, FL 33701, USA
[4]College of Marine Science, University of South Florida, St. Petersburg, FL 33701, USA
[5]Cooperative Institute for Marine and Atmospheric Studies, University of Miami, Miami, FL 33149, USA
[6]NOAA Atlantic Oceanographic and Meteorological Laboratory, 4301 Rickenbacker Causeway, Miami 33149, USA
[7]Marine Sciences, The University of Trinidad and Tobago, TT, Trinidad and Tobago
[8]National Commission for Knowledge and Use of Biodiversity (CONABIO), Mexico City, 14010, Mexico
[9]UAV Collaborative, Moffett Field, CA 94035, USA

ABSTRACT: Diurnal variation of net community production (NEP) and net community calcification (NEC) were measured in coral reef and seagrass biomes during October 2012 in the lower Florida Keys using a mesocosm enclosure and the oxygen gradient flux technique. Seagrass and coral reef sites showed diurnal variations of NEP and NEC, with positive values at near-seafloor light levels >100–300 µEinstein $m^{-2}$ $s^{-1}$. During daylight hours, we detected an average NEP of 12.3 and 8.6 mmol $O_2$ $m^{-2}$ $h^{-1}$ at the seagrass and coral reef site, respectively. At night, NEP at the seagrass site was relatively constant, while on the coral reef, net respiration was highest immediately after dusk and decreased during the rest of the night. At the seagrass site, NEC values ranged from 0.20 g $CaCO_3$ $m^{-2}$ $h^{-1}$ during daylight to –0.15 g $CaCO_3$ $m^{-2}$ $h^{-1}$ at night, and from 0.17 to –0.10 g $CaCO_3$ $m^{-2}$ $h^{-1}$ at the coral reef site. There were no significant differences in pH and aragonite saturation states ($\Omega_{ar}$) between the seagrass and coral reef sites. Decrease in light levels during thunderstorms significantly decreased NEP, transforming the system from net autotrophic to net heterotrophic.

KEY WORDS: Coral reef · Seagrass · Production · Calcification · Florida Keys



## INTRODUCTION

Photosynthesis, respiration, calcification, and excretion as well as uptake and recycling of nutrients are major metabolic processes involved in carbon turnover in all ecosystems (Langdon & Atkinson 2005). Net community production (NEP), the difference between gross production and respiration, is a measure of how well a system maintains biomass. Similarly, the difference between gross community calcification and calcium carbonate dissolution is defined as net community calcification (NEC) (Andersson & Gledhill 2013). Together with other constructive (e.g. carbonate sediment accumulation, cementation, and reef growth) and destructive (e.g. sediment loss due to erosion and transport, dissolution of carbonate sediment, loss of calcifying organisms) processes, NEC determines whether or not coral reefs maintain structural complexity over long periods of time (e.g. years). An important question is how these processes balance each other in tropical, shallow-water coral reef and seagrass ecosystems (Hatcher 1997).

*Corresponding author: daniela.turk@dal.ca

On shorter time scales, NEP and NEC vary with community composition and ambient conditions, for example light, temperature, nutrients, seawater chemistry and hydrographic regime that influences temperature and seawater chemistry (Langdon & Atkinson 2005). NEP and NEC can in turn also influence the chemistry of ambient water. Waters adjacent to coral reefs and seagrass beds show variations at a range of temporal scales (from hours to years). Diurnal changes in NEP and NEC and associated changes in pH, dissolved oxygen (DO), and partial pressure of $CO_2$ ($pCO_2$) of waters adjacent to coral reef organisms were first measured more than 60 yr ago (Seargent & Austin 1954, Odum & Odum 1955, Smith 1973). More recently, these variations have been further described by several others (Kayanne et al. 2005, Yates & Halley 2006, Manzello 2010, Anthony et al. 2011, Kleypas et al. 2011, McGillis et al. 2011, Santos et al. 2011, Gray et al. 2012, Price et al. 2012, Smith et al. 2013). Fluctuations in these chemical parameters have also been observed in seagrass beds (Invers et al. 1997, Marbà et al. 2006, Buapet et al. 2013) as well as other benthic community environments where the biologically active surface area is sufficiently large relative to the water volume (per unit time). Positive NEP and NEC and increased oxygen concentration and pH are typically reported during daylight and the opposite pattern occurs during the dark. In open water systems, highest pH and DO, and lowest $pCO_2$ values are typically observed around mid-day, when photosynthesis is at a maximum. In systems with long water residence times, pH and DO values tend to rise through daylight hours, with a peak observed closer to twilight. During such maxima, carbonate mineral saturation states also reach their highest values (Yates et al. 2007, Shamberger et al. 2011). How much the ambient water chemistry changes, however, is a complex function of the physical forcing (e.g. circulation, light), morphology, and benthic metabolism (Smith et al. 2013).

The diurnal cycle in benthic metabolism is also affected by short-term (hours) weather events (Lawrence et al. 2004, Falter et al. 2011, Naumann et al. 2013). Rapid declines in incident light during tropical storms result in a temporary decrease in gross primary production and respiration, altering the balance between production and respiration in coral reefs (Falter et al. 2011). Naumann et al. (2013) also observed a significant decline in benthic net production, gross production and respiration following a storm. During a wind event in Florida Bay, Lawrence et al. (2004) reported suspension of bottom sediments, injection of nutrients and reduced light that had an effect on benthic metabolism and resulted in a strongly heterotrophic water column. Coral reef NEC also decreases as ambient light decreases (Langdon & Atkinson 2005, Shamberger et al. 2011, Albright et al. 2013). This can lead to net dissolution during storms in daylight, under high cloud cover and high turbidity (Yates & Halley 2006). More information regarding the influence of tropical storms on NEP and NEC in coral reef and seagrass environments is needed.

There is growing interest in understanding whether calcification and production rates in shallow water tropical coral reefs and seagrass beds may be affected by long-term ocean pH changes, such as those related to the increase of carbon dioxide in the atmosphere (Langdon et al. 2000, Jury et al. 2010). Coral reef NEC can decrease with increasing ambient seawater $pCO_2$ and decreasing aragonite saturation ($\Omega_{ar}$) (Langdon & Atkinson 2005, Yates & Halley 2006, Kleypas & Yates 2009, Silverman et al. 2009, Fabricius et al. 2011, Shamberger et al. 2011). Langdon et al. (2000) suggest a 40% decrease (relative to pre-industrial level) in coral calcification rates by 2065 due to the effect of rising $pCO_2$ and temperature on saturation state. 'Critical threshold values' of $pCO_2$ and $\Omega_{ar}$ at which calcium carbonate ($CaCO_3$) gains and losses by dissolution are balanced, and no reef growth occurs (i.e. NEC = 0) have been defined (Andersson & Gledhill 2013). Yet, the studies cited above show a large variability in measurements of threshold values, as marine organisms seem to have a broad range of reactions to ocean warming and acidification. Therefore, pre-defined 'critical threshold values' in mixed reef communities are not well established.

While coral reefs might be negatively impacted by a long-term increase in ocean acidification, seagrasses might benefit by increased $pCO_2$ (Palacios & Zimmerman 2007). Seagrass beds may even mitigate ocean acidification impacts on adjacent coral reefs by utilizing large amounts of inorganic carbon and increasing pH in the ambient water (Doney et al. 2009, Semesi et al. 2009, Manzello et al. 2012, Andersson & Gledhill 2013). A recent study shows that increases in ambient pH of up to 0.38 units and a corresponding increase in $\Omega_{ar}$ of up to 2.9, are possible in coral reefs near seagrass meadows (Unsworth et al. 2012). However, this study was based on calculations of seasonal changes in seagrass NEC from hypothetical residence times and lacking supporting physical data from real seagrass communities. More observations are needed to determine whether seagrass beds can affect pH on spatial and temporal scales large enough to counter the impacts of rising atmospheric $CO_2$.

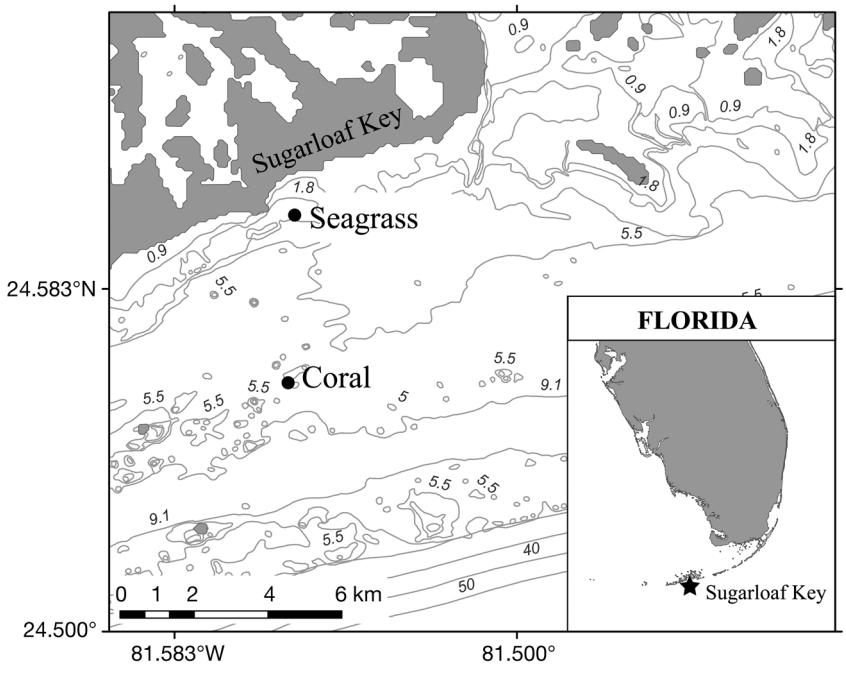


Fig. 1. Study sites (seagrass and coral reef) off Sugarloaf Key, Florida, USA, with bathymetry (in meters)

Previous studies have estimated coral community NEP and NEC using various methods, including flow respirometry (Marsh & Smith 1978, Gattuso et al. 1999), closed controlled volume enclosures (Yates & Halley 2003, Falter et al. 2011, Smith et al. 2013), open controlled volumes (Kline et al. 2012, Gattuso et al. 2014), boundary layer gradient flux (GF) methods (McGillis et al. 2011), and eddy correlation (EC) techniques (Long et al. 2013). Estimates of reef carbonate dynamics have been further extended to larger regional scales using remote sensing [Brock et al. 2006a,b, Moses et al. 2009). Moses et al. (2009) used high spatial resolution Landsat-7/ETM+ images to determine that over the 2711 $km^2$ of the North Florida Reef Track, gross production totaled 3.01 × $10^9$ kg C $yr^{-1}$, and calcification totaled –1.68 × $10^6$ kg CaCO3 $yr^{-1}$. However, at present, the understanding of the spatial and temporal variability of carbonate chemistry within coral reef and seagrass environments remains rudimentary.

In this study, we examined short-term (hourly to daily) NEP and NEC in adjacent coral reef and seagrass environments near Sugarloaf Key, in the Lower Florida Keys during October 2012. The main objectives of the study were to (1) describe and compare community production and calcification (i.e. metabolism) rates in each habitat across a diel cycle, (2) estimate the compensation light intensity for NEP and NEC for each habitat, and (3) to define 'critical threshold values' of seawater $pCO_2$, $\Omega_{ar}$, and NEP for NEC.

Our approach included the use of the Submersible Habitat for Analyzing Reef Quality (SHARQ) benthic chamber system (Yates & Halley 2003, 2006), complemented by vertical dissolved oxygen gradient measurements using a Coral Reef Oxygen Sensing Systems (CROSS) (McGillis et al. 2011). The automated CROSS system was moored at the coral reef site, and thus it allowed extending observations for 2 d beyond the SHARQ deployment while also providing a separate, independent measure of NEP. This enabled us to investigate the influence of ambient light changes during episodic tropical storm events on NEP and NEC. Our short-term study provides baseline information on community metabolism in 2 adjacent habitats of the Lower Florida Keys.

## MATERIALS AND METHODS

Our study focused on a shallow coral reef (24° 33.698' N, 81° 33.296' W) and a seagrass site (24° 35.989' N, 81° 33.263' W) on the Atlantic Ocean flank of the Lower Florida Keys, immediately south of Sugarloaf Key (Fig. 1). The seagrass site was located closer to shore at about 3.6 m depth. The seagrass bed consisted primarily of the species *Thallassia testudinum* with blade length of approx. 20 cm and density ranging from 210 to 690 g DW $m^{-2}$ (Yarbro et al. 2013). Calcareous algae including *Penicillus* sp. and *Halimeda* sp. were interspersed throughout the seagrass bed. The coral reef site was at 5 m depth. A 25 m long transect was established at the coral reef site in close approximation to the SHARQ and CROSS. The percent cover for different benthic groups were calculated based on images taken along this transect using the software Coral Point Count with Excel extensions (CPCe; Point Count'99, http://prosper.cofc.edu/~coral/corallab.htm). The benthos was assigned to 1 of 5 main categories: live coral (25%); dead coral with algae (7%); algae (including macroalgae, and other live) (3%); $CaCO_3$ substrate including sand, pavement, rubble (20%); and 'other', including sponges, gorgonians, zoanthids and unknowns (45%). The estimated total live coral cover was 25%, with the predominant species including boulder coral types (*Orbicella annularis* [12%],

*Montastraea cavernosa* [4.5%], *Orbicella faveolata* [4.5%], *Siderastrea sidereal* [3%], and *Colpophyllia natans* [1%]), and sparse occurrence of other species. Specific observations on coral conditions were not performed; however, the photos suggest that all coral species were visually healthy with no signs of bleaching or disease.

Both the coral reef and seagrass sites were instrumented with conductivity-temperature SBE 37 MicroCat C-T sensors. A Recording Doppler Current Profiler (RDCP 600 – Aanderaa) was deployed at the seagrass site, and an Argonaut-XR multi-cell Doppler current profiler (Sontek) was deployed at the coral reef site. Both ADCP's measured vertical profiles of horizontal current speed and direction in bin sizes of 1 m from the bottom to approx. 1 m below the surface, at 10 min intervals. Throughout this study, a Davis Instruments Vantage Pro Plus Wireless Weather Station was mounted onboard the research vessel anchored on the coral reef site. This weather station was equipped with a rain collector, temperature and humidity sensors, anemometer, and incoming solar photosynthetically active radiation (PAR) sensors. All the sensors were located on a mast at 10 m above the sea level and 5 m above the boat's highest structure to avoid interference.

### SHARQ enclosure

Community metabolism (NEP and NEC) rates in each habitat were measured using a Submersible Habitat for Analyzing Reef Quality (SHARQ) benthic chamber system (Yates & Halley 2003, 2006). Two adjacent SHARQ incubation chambers (11 $m^2$ each) were deployed by SCUBA divers at approx. 3.6 m depth at the seagrass site on October 16 and 17, 2012, and approx. 5 m depth at the coral reef site from October 19 to 21, 2012. Chemical parameters were monitored throughout the day and night using a shipboard flow-through analytical system connected to the chamber in a closed loop system (Yates & Halley 2003). Measurements in ambient water outside of the chambers were made using the same flow-through analytical system disconnected from the chamber with the intake located at the same depth near the seafloor. Dissolved oxygen (±0.1 mg $l^{-1}$), temperature (±0.01°C), and salinity (±0.01) were measured at 1 min intervals using a YSI dissolved oxygen meter with a pressure compensated field probe and a flow-through Falmouth Scientific ETSG, respectively. Water samples for total alkalinity (TA) (±1 µmol $kg^{-1}$), spectrophotometric pH (±0.005), and total $CO_2$ ($TCO_2$) (±3 µmol $kg^{-1}$) were collected from the flow through system every 4 h throughout incubation periods. Spectrophotometric pH was measured immediately following sample collection in the field using an Ocean Optics USB2000 spectrometer and the methods of Zhang & Byrne (1996). TA was measured spectrophotemetrically with an Ocean Optics USB2000 spectrometer using the technique in Yao & Byrne (1998). Total carbon was determined via carbon coulometry with a CM5014 carbon coulometer and CM5130 acidification module as described by Dickson et al. (2007). The remaining carbonate system parameters (including inorganic carbon speciation and $pCO_2$) were calculated using the seawater carbon speciation program CO2SYS (Pierrot et al. 2006), dissociation constants for the carbonate system, K1 and K2 from Mehrbach et al. (1973) refit by Dickson & Millero (1987), $K_{HSO4}$ from Dickson (1990), and using the total pH scale ($pH_T$). Photosynthetically active radiation (PAR) was measured in air above the sea surface and at the seafloor outside of the chamber using LiCOR 2pi and 4pi PAR sensors. The exact volume of each SHARQ chamber at each location was determined by dilution of a known quantity of fluorescein dye measured using a Turner Instruments SCUFA Fluorometer (Yates & Halley 2003).

The flow-through systems of each incubation chamber were connected to a gas equilibration chamber located on the vessel at the surface. These gas equilibrators were used during 4 to 6 h each night to equilibrate water inside of the chamber with atmospheric $pCO_2$ and $O_2$ to mitigate $CO_2$ build-up and $O_2$ depletion inside of the chambers during incubations.

Net community production, $NEP_{SHARQ}$ (mmol $O_2$ $m^{-2}$ 15 $min^{-1}$), was calculated at 15 min time intervals (the approximate water residence time inside of the incubation chamber) throughout incubation periods using equations from Yates & Halley (2003) as:

$$NEP_{SHARQ} = \Delta DO \frac{SHARQ_{volume}}{SHARQ_{area}} \quad (1)$$

where ΔDO (mmol $O_2$ $m^{-3}$ 15 $min^{-1}$) is the change of dissolved $O_2$ concentration in the enclosure over a 15 min time interval and $SHARQ_{volume}$ and $SHARQ_{area}$ are volume ($m^3$) and surface area ($m^2$) of the basal portion of the enclosure, respectively. $NEP_{SHARQ}$ (mmol $O_2$ $m^{-2}$ 15 $min^{-1}$) was converted to mmol $O_2$ $m^{-2}$ $h^{-1}$ for comparison with CROSS estimates.

Net community calcification, $NEC_{SHARQ}$ (mmol $CaCO_3$ $m^{-2}$ 4 $h^{-1}$), was calculated at a 4 h intervals within each 24 h incubation period (14 measurements at the seagrass site and 16 at the coral reef site). The alkalinity anomaly technique of Smith &

Key (1975) and equations from Yates & Halley (2003) were used:

$$NEC_{SHARQ} = 0.5\Delta TA \frac{SHARQ_{volume}}{SHARQ_{area}} \quad (2)$$

where ΔTA (mmol $m^{-3}$ 4 $h^{-1}$) is the change of TA in the enclosure over a 4 h time interval. Photosynthetic quotient (PQ) for seagrass and coral reef over 4 h time intervals was calculated as:

$$PQ = \frac{\Delta DO}{\Delta(TCO_2 - 0.5TA)} \quad (3)$$

### CROSS chemical boundary layer method

At the coral reef site, NEP was also determined by vertical dissolved oxygen gradient measurements using a Coral Reef Oxygen Sensing System (CROSS) (McGillis et al. 2011). A CROSS system was deployed at the coral reef site at ~5 m depth from October 16 to 21, 2012. The CROSS system included 4 (2 sets of 2) Aanderaa Optode dissolved $O_2$ concentration sensors, which were positioned at approx. 0.2 m and 0.9 m above the sea floor. Each sensor collected $O_2$ data at 10 s intervals. A SeaFET pH sensor (Satlantic LP) was mounted on the CROSS frame adjacent to the 2 lower $O_2$ sensors, at 0.2 m above the reef. The SeaFET was calibrated prior to deployment via a single-point, spectrophotometric pH determination using an *m*-cresol purple stock solution prepared from purified indicator at the University of South Florida (Laboratory of Dr. Robert Byrne, courtesy of Mark C. Pastavas) (Liu et al. 2011). The SeaFET was re-calibrated following the experiment using Tris buffer certified reference material (CRM, $CO_2$ Quality Control Group, Scripps Institute of Oceanography) over the temperature range of 5 to 35°C at 5°C intervals (Dickson et al. 2007). CROSS data extended time series of NEP provided by SHARQ at the coral reef site and enabled us to capture changes in NEP, $O_2$, and pH during 3 storm events. The comparison between SHARQ and CROSS methods is described in more detail in McGillis et al. (2011).

$NEP_{CROSS}$ (mmol $O_2$ $m^{-2}$ $h^{-1}$) was calculated using an estimate of eddy diffusivity, $K_z$, expressed as $K_z = u_*\kappa z$, and the vertical concentration gradient in $O_2$ (dDO/d*z*) as follows from (McGillis et al. 2011):

$$NEP_{CROSS} = u_*\kappa \frac{(DO_{z=2} - DO_{z=1})}{\ln(z_2 / z_1)} \quad (4)$$

where $u_*$(cm $s^{-1}$) is the friction velocity, κ is the von Karman constant (0.41), and $DO_z$ is the dissolved $O_2$ concentration (mmol $m^{-3}$). $DO_{z=1}$ and $DO_{z=2}$ are values averaged over 10 min from the 2 sets of Aanderaa optodes at 0.9 ($z_1$) and 0.2 ($z_2$) m above the seafloor, respectively. The $u_*$ estimate was derived from the moored ADCP data using a logarithmic law technique (Wimbush & Munk 1970; see the Supplement at www.int-res.com/articles/suppl/m538p035_supp.pdf). The mean (± SD) value of $u_*$ of 1.52 ± 0.82 cm $s^{-1}$ was used for estimation of $NEP_{CROSS}$ and its uncertainty. Our mean $U_0/u_*$ of 0.17 ± 0.07 using the average water column velocity as a reference $U_0$ is slightly higher than the values of 0.10 to 0.14 measured by previous studies (Reidenbach et al. 2006, McGillis et al. 2011). We expect that friction on benthic topography would slow down current speed closer to the sea floor compared to 1 m above the sea floor—in particular in coral reef environments and hence our value of $u_*$ may be overestimated. The uncertainly in our estimation of $u_*$ would have been significantly lowered by using a current meter (not available for this study) designed for resolving the water column velocity profile (McGillis et al. 2011).

### $\Omega_{ar}$, $pCO_2$, and NEP thresholds and the compensation light intensities

The $pCO_2$, $\Omega_{ar}$, and NEP 'critical threshold values', and light compensation intensity for $NEC_{SHARQ}$ (i.e. the values at which rates of calcification and dissolution are equivalent) as well as the response of NEC to these 4 environmental variables (slope of the fitted regression) were determined by univariate linear regressions of NEC vs. $pCO_2$, $\Omega_{ar}$, NEP and PAR. The 'threshold' was defined as the point at which the fitted regression line crosses zero on the y-axis ($NEC_{SHARQ}$ = 0), for each of the variables.

In addition, we performed multiple linear regressions analyses (full model) to assess the combined influence of all 4 explanatory environmental variables ($pCO_2$, $\Omega_{ar}$, NEP and PAR) on NEC in each habitat. Furthermore, to determine significant differences in the response of NEC to these variables in the different habitats, the data from both habitats was combined and habitats were treated (seagrass or coral reef) as a factor, i.e. an (0,1) indicator variable. The model regressed NEC on the environmental variables ($pCO_2$, $\Omega_{ar}$, NEP and PAR), as well as habitat. It also included the interaction of habitat with each of the environmental variables. If these interaction terms are significant ($p < 0.1$), the implication is that the response of NEC to the environmental variables (the slope) depends on habitat. The effect

of the SHARQ chamber was also assessed by including chamber as an indicator (0,1) variable within the regression analyses. In all cases, the chamber effect was found to be negligible (large p-values) and thus replicate data from Chambers 1 and 2 were pooled for all analyses. The regression residuals were examined for all analyses; and they implied that the regression assumptions were being met.

Finally, regression variable selection was carried out to determine which of the 4 variables was most important for prediction of NEC (forward selection, backward elimination, and stepwise regression using the Akaike Information Criterion [AIC]).

The compensation light intensity for NEP at both habitats was defined as the value of PAR measured at the seafloor adjacent to SHARQ chambers, at which $NEP_{SHARQ}$ and $NEC_{SHARQ}$ equal zero. By analogy to photosynthesis-irradiance (*P-I*) curves (Platt et al. 1980), we plotted $NEP_{SHARQ}$ vs. PAR and fitted the model, as follows:

$$NEP = P_{max}(1 - e^{-\alpha \cdot PAR/P_{max}}) - R \quad (5)$$

We estimated the unknown $P_{max}$, α and $R$, where $P_{max}$ is the maximum photosynthetic rate, α is the initial slope at low PAR and $R$ is respiration rate (see Fig. 8). Furthermore, we defined the quantity, $NEP_{max}$, to be the fitted maximum photosynthetic rate reduced by the respiration rate ($P_{max}$–$R$) and estimated the compensation and saturation light intensity, $I_c$ and $I_s$, respectively. We did not have adequate data to justify the Eq. (5) fit to $NEC_{SHARQ}$ vs. PAR; thus, we applied linear regression to determine light compensation intensity for NEC as described above.

## RESULTS

### Environmental parameters within the SHARQ enclosure and ambient water

Discrete water measurements from within the SHARQ chambers showed similar temperatures during the study at both sites. The seagrass site showed slightly higher salinity than the coral reef site (Fig. 2, Table 1). Diurnal cycles for the DO and inorganic carbon parameters were observed at both sites. High DO, pH (Fig. 2) and $\Omega_{ar}$ (Fig. 3) occurred during daylight hours and low values at night. $TCO_2$, TA and $pCO_2$ (Fig. 3) showed the opposite pattern. At the seagrass site, the highest DO, pH and $\Omega_{ar}$ and the lowest $TCO_2$, TA and $pCO_2$ within SHARQ chambers were observed at 19:00 h. The maximum day-night differences were: DO(Δ~17 m μM), TA (Δ ~50 μmol $kg^{-1}$), $TCO_2$ (Δ ~145 μmol $kg^{-1}$), and pH (Δ ~0.23). Aragonite saturation states ranged between 2.5 and 3.9, and $pCO_2$ between 336 and 656 μatm. At the coral reef site, the highest DO, pH and $\Omega_{ar}$ and the lowest $TCO_2$, TA and $pCO_2$ within SHARQ chambers were observed at 15:00 h, and the maximum day-night differences were: DO (Δ ~220 μM), TA (Δ ~70 μmol $kg^{-1}$), $TCO_2$ (Δ ~150 μmol $kg^{-1}$) and pH (Δ ~0.21). $\Omega_{ar}$ at the coral reef site ranged between 2.7 and 4.1 and $pCO_2$ between 321 and 627 μatm.

Discrete water measurements of temperature, salinity, DO and inorganic carbon data in the ambient water outside the SHARQ chambers included 5 measurements at 2 depths (0.2 and 0.9 m above the seafloor) at the seagrass site and 7 measurements from the same depths at the coral reef site (Figs. 2 & 3, blue). These data showed small average differences from SHARQ chamber measurements (salinity = –0.5, temperature = +0.09°C, DO = +0.1 μM, TA = –23 μmol $kg^{-1}$, $TCO_2$ = –7 μmol $kg^{-1}$, pH = +0.005, $pCO_2$ =

Table 1. Discrete carbonate and physical parameters measured at 3.6 m depth at the seagrass (16 and 17 October 2012) and at 5 m depth at the coral reef site (19 to 21 October 2012) within Submersible Habitat for Analyzing Reef Quality (SHARQ) chambers (range or mean ± SD; n = 16 for seagrass [8 per chamber] and n = 24 for coral reef [12 per chamber]), compared to Manzello et al. (2012) salinity and carbonate parameters at the nearby locations during autumn of 2010 and 2011. DO: dissolved oxygen; TA: total alkalinity; $TCO_2$: total carbon dioxide; $TA_n$ and $TCO_{2n}$ are TA and $TCO_2$ values normalized to average salinity; $\Omega_{ar}$: aragonite saturation; $pCO_2$: partial pressure of $CO_2$; NEP: net community production; NEC: net community calcification. Blank cells: no data

| Parameter | Present study | | Manzello et al. (2012) | |
|---|---|---|---|---|
| | Seagrass site | Coral reef | Seagrass site | Coral reef |
| Temperature (°C) | 28.0 ± 0.2 | 28.4 ± 0.2 | | |
| Salinity | 36.6 ± 0.1 | 36.2 ± 0.1 | 36.22 | 35.40 |
| DO (ml $l^{-1}$) | 6.1 ± 1.4 | 5.8 ± 1.2 | | |
| TA (μmol $kg^{-1}$) | 2193 ± 19 | 2278 ± 23 | 2056.3 | 2023.7 |
| $TCO_2$ (μmol $kg^{-1}$) | 1928 ± 56 | 1984 ± 39 | 1987.7 | 2001.4 |
| $TA_n$ (μmol $kg^{-1}$) | 2178 ± 16 | 2293 ± 24 | 2367.4 | 2360.9 |
| $TCO_{2n}$ (μmol $kg^{-1}$) | 1915 ± 54 | 1997 ± 40 | 2288.2 | 2334.5 |
| pH | 7.97 ± 0.09 | 8.02 ± 0.05 | | |
| $\Omega_{ar}$ | 3.2 ± 0.5 | 3.6 ± 0.3 | | |
| $pCO_2$ (μatm) | 471 ± 115 | 423 ± 67 | | |
| $NEP_{SHARQ}$ (mmol $O_2$ $m^{-2}$ $h^{-1}$) | –6.2 to 12.3 | –12.5 to 8.6 | | |
| $NEC_{SHARQ}$ (g $CaCO_3$ $m^{-2}$ $h^{-1}$) | –0.15 to 0.2 | –0.10 to 0.17 | | |

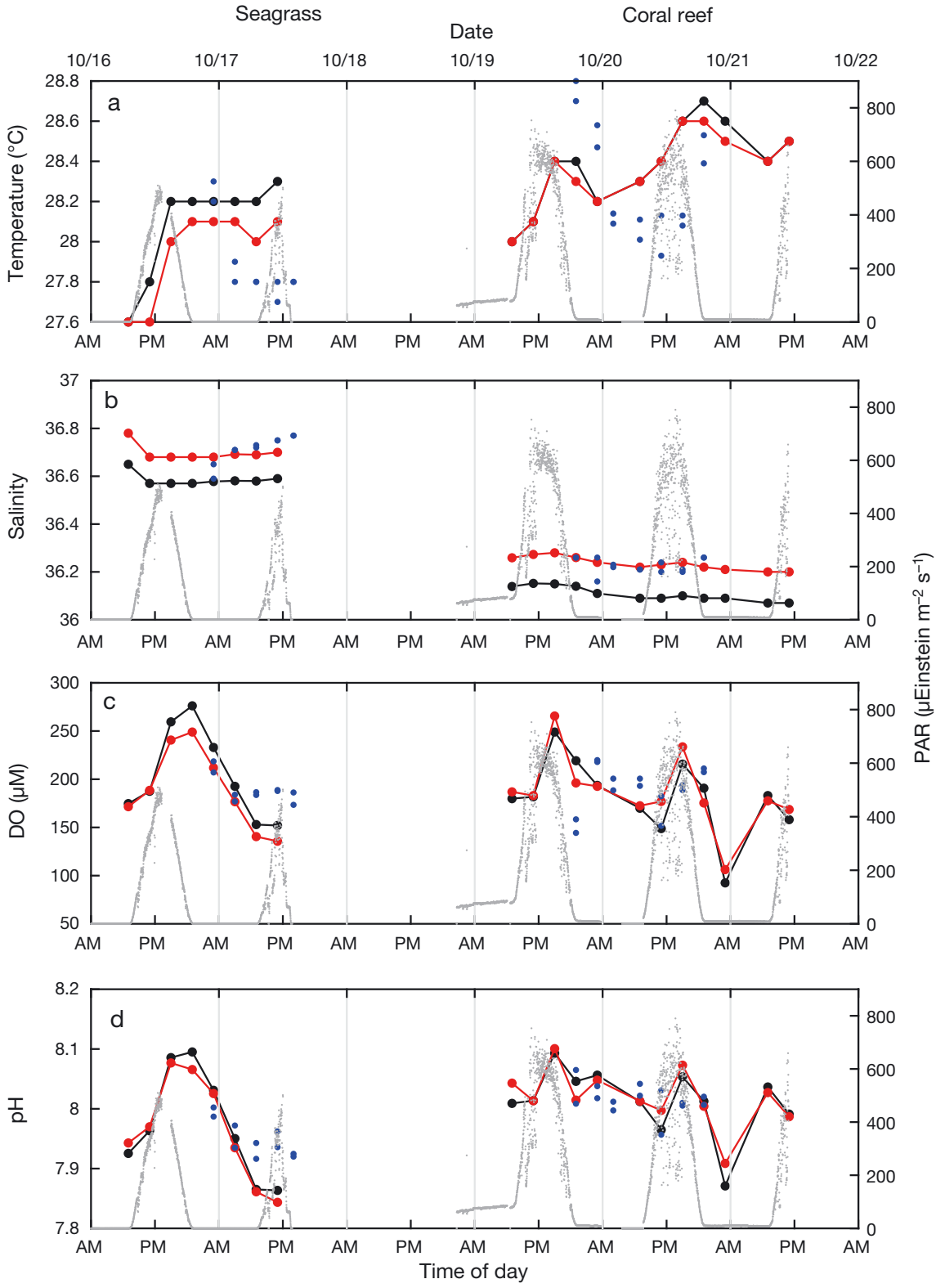


Fig. 2. Discrete (a) temperature (°C), (b) salinity, (c) dissolved oxygen (DO) (µM) and (d) pH measured in 2 Submersible Habitat for Analysing Reef Quality (SHARQ) chambers (Chamber 1: red, Chamber 2: black) and ambient water (blue) at the seagrass site on October 16 and 17, 2012 and the coral reef site from October 19 to 21, 2012. AM and PM indicate midnight and noon, respectively. Photosynthetically active radiation (PAR; µEinstein m$^{-2}$ s$^{-1}$) at the seafloor outside the chambers (grey dots) is also shown

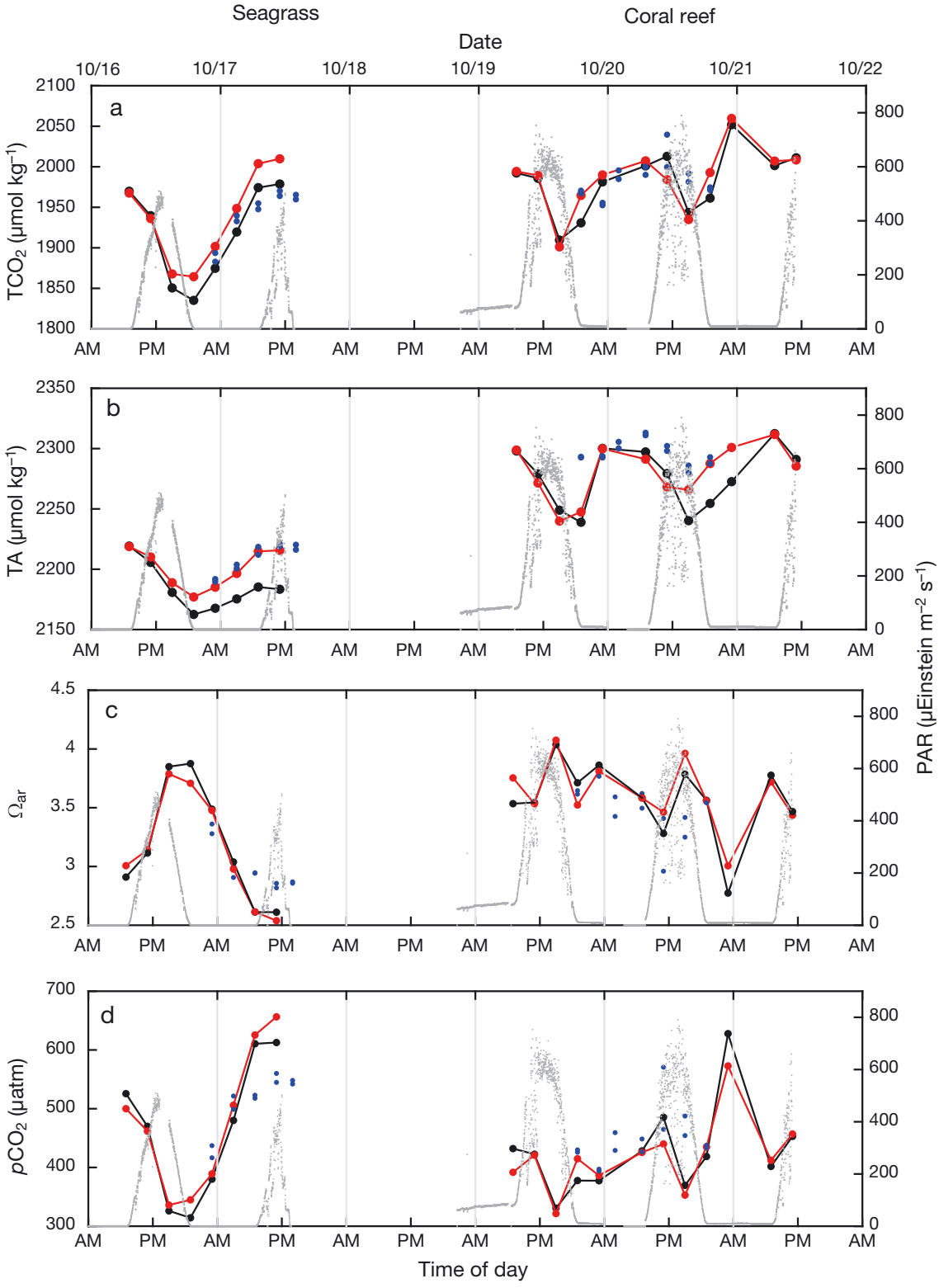


Fig. 3. Discrete (a) total carbon dioxide ($TCO_2$; (µmol $kg^{-1}$), (b) total alkalinity (TA; µmol $kg^{-1}$), (c) aragonite saturation state ($\Omega_{ar}$) and (d) partial pressure of $CO_2$ ($pCO_2$; µatm) measured in 2 Submersible Habitat for Analysing Reef Quality (SHARQ) chambers (Chamber 1: red, Chamber 2: black) and ambient water (blue) at the seagrass site on October 16 and 17, 2012 and the coral reef site from October 19 to 21, 2012. AM and PM indicate midnight and noon, respectively. Photosynthetically active radiation (PAR; µEinstein $m^{-2}$ $s^{-1}$) at the seafloor outside the chambers (grey dots) is also shown

−27 µatm, and $\Omega_{ar}$ = +0.1). PAR measured at the seafloor adjacent to the chambers (Figs. 2 & 3, grey) at both the seagrass and coral reef sites showed a typical daily pattern of maximum values of 500 µEinstein $m^{-2}$ $s^{-1}$ at the seagrass site and 800 µEinstein $m^{-2}$ $s^{-1}$ at the coral reef site.

### Ambient water conditions at the coral reef site

The moored sensors at the coral reef site showed that from 16 to 21 October 2012, temperature and salinity at 5 m depth in the coral reef site ranged from 27.9 to 28.5°C and 36.04 and 36.33, respectively (Fig. 4a). Salinity decreased during mid-day on October 18 along with temperature, and then values for both variables increased again. Tidal variation at the coral reef site led to pressure variations of 5.56 to 6.38 dbar. Current speed values were between 4 and 18 cm $s^{-1}$ on October 16 and 17 and between 0.4 and 12 cm $s^{-1}$ from October 18 to 21 (Fig 4b).

Solar radiation (Fig. 4c) from ship-mounted sensors at the coral reef site shows typical daily variation, with short intense variations introduced by thunderstorms. The PAR sensor mounted at the seafloor outside the SHARQ chamber at the seagrass site also detected this variability associated with thunderstorms (Figs. 2 & 3). Two daytime storms occurred during the study, the first on October 17, with up to 9.1 mm of rain, and a weaker storm on October 18 with 1.5 mm of rain. Another storm occurred during the night of October 18 with 4.1 mm of rain. Storms caused a rapid decrease in ambient solar radiation by attenuation due to clouds. During one storm, PAR decreased from 3900 to 0 µEinstein $m^{-2}$ $s^{-1}$, and during another from 2295 to 459 µEinstein $m^{-2}$ $s^{-1}$ (Fig. 4c).

An average value of $O_2$ measurements from 2 lower optodes and pH

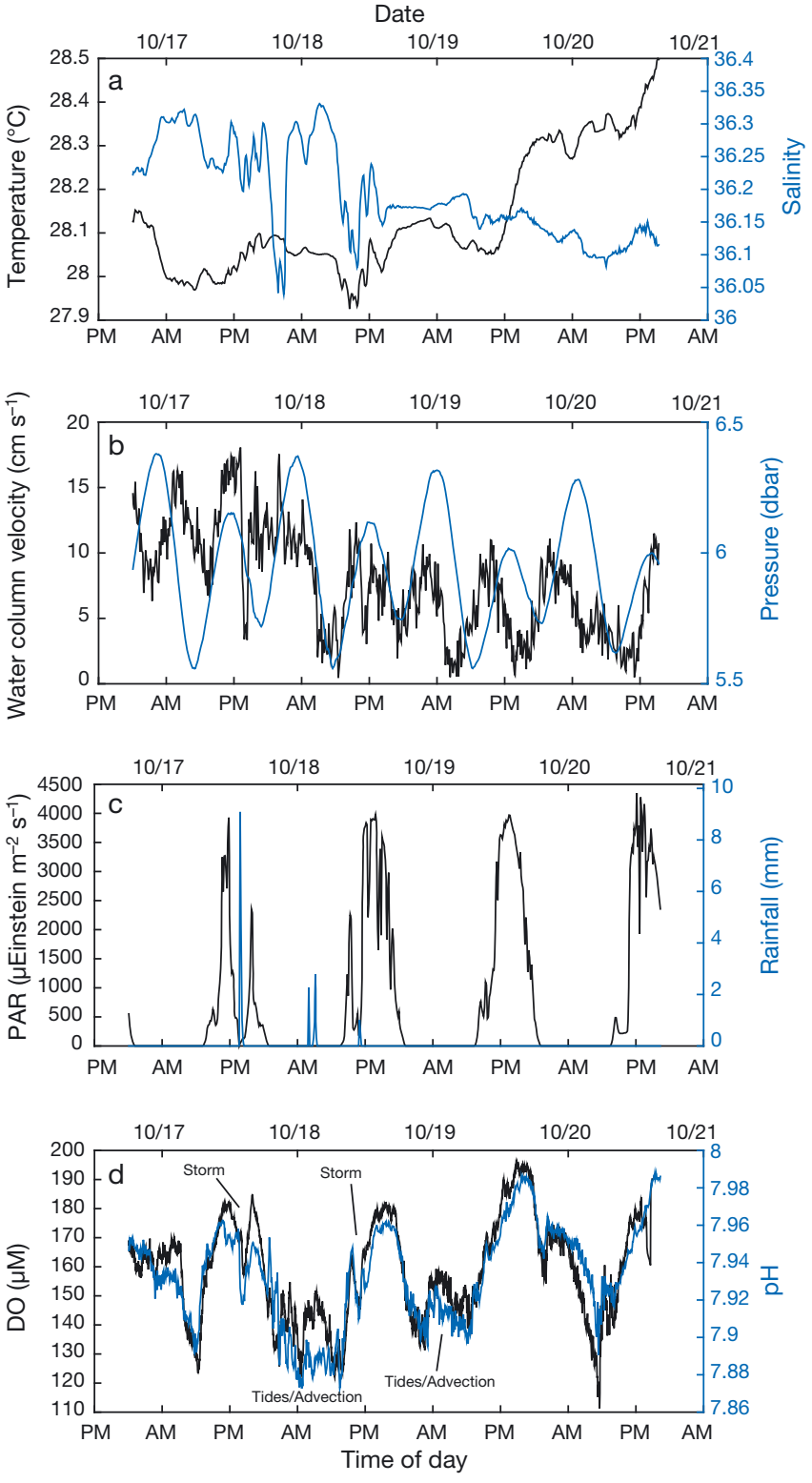


Fig. 4. Time series of ambient water conditions at the coral reef site: (a) temperature (°C) and salinity, (b) current speed (cm $s^{-1}$) and pressure (dbar) obtained at 5 m depth, (c) PAR above the surface (µEinstein $m^{-2}$ $s^{-1}$) and rainfall (mm), and (d) average value of dissolved oxygen (DO; µM) measured by the 2 sensors at 0.2 m above the reef and pH, from October 16 to 21, 2012

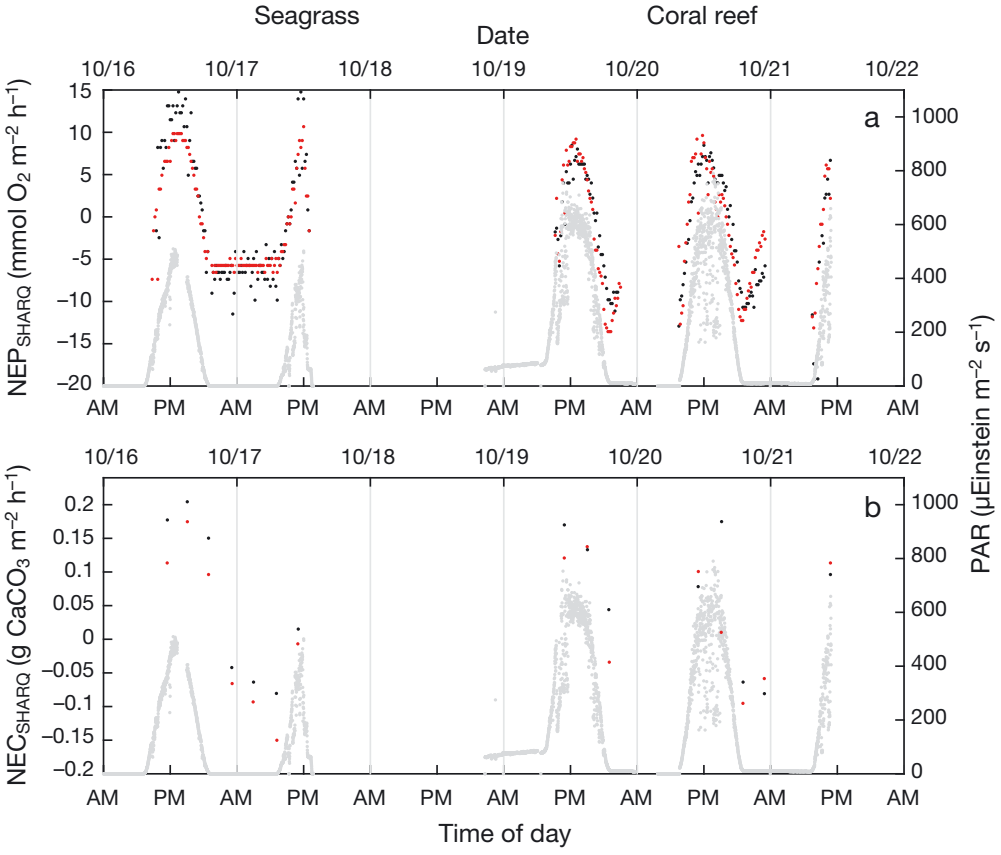


Fig. 5. (a) $NEP_{SHARQ}$ (mmol $O_2$ $m^{-2}$ $h^{-1}$) and (b) $NEC_{SHARQ}$ (g $CaCO_3$ $m^{-2}$ $h^{-1}$) from 2 chambers (Chamber 1: red dots, Chamber 2: black dots) and PAR (µEinstein $m^{-2}$ $s^{-1}$, grey dots) at the seafloor outside the chambers at the seagrass site on October 16 and 17, 2012 and at the coral reef site from October 19 to 21, 2012

from the SeaFET positioned on CROSS at 0.2 m above the reef are presented in Fig. 4d. Both time series showed a typical diurnal pattern with values increasing during the day and decreasing during the night. DO varied between 110 and 195 µM, and pH between 7.87 and 7.99. At night, the average $O_2$ concentrations obtained from 2 sensors positioned at 0.2 m above the reef were lower than those from the optodes positioned at 0.9 m above the reef (not shown). This reflects net respiration (negative NEP) consuming oxygen closer to the reefs at night. During daytime, the values closer to the reef were higher due to oxygen production by photosynthesis. Our data also show smaller increases in DO (25 µM) and pH (0.02) during the night. A discrepancy of 0.05 to 0.1 was noted between SeaFET pH and pH determined spectrophotometrically at the coral reef site. We believe that this was systematic over the short deployment but that it did not affect the pattern of diurnal pH variability.

Contemporaneously with the decrease in solar radiation and high rainfall during daytime storms on mid-day October 17 and mid-day October 18 (Fig. 4c), sudden decreases in $O_2$ (25 and 20 µM, respectively) and pH (0.02) at 0.2 m above the coral reef were observed. The oxygen values closer to the corals decreased below the values at the upper optode. During the night storm, the upper oxygen concentrations decreased (not shown), while the lower oxygen concentrations and pH slightly increased.

At the coral reef site, a high degree of correlation with no lag was observed for pH and $O_2$ ($r^2$ = 0.87), and pH and solar radiation ($r^2$ = 0.65). Correlations were lower between pH and temperature ($r^2$ = 0.42), salinity ($r^2$ = –0.34), and pressure ($r^2$ = –0.004) or current speed ($r^2$ = 0.0024) (with or without lag).

### Net community production ($NEP_{SHARQ}$ and $NEP_{CROSS}$)

$NEP_{SHARQ}$ showed diurnal cycles that matched incident PAR measured at the seafloor adjacent to the chambers at both the seagrass and coral reef sites (Fig. 5a). Positive NEP was observed during the seagrass deployment from 08:00 to 19:00 h on October 16 with average highest values from the 2 chambers reaching close to 12.3 ± 1.0 mmol $O_2$ $m^{-2}$ $h^{-1}$ near 12:00 h, when PAR reached maximum values of 500 µEinstein $m^{-2}$ $s^{-1}$. On October 17, NEP was positive from 07:00 to 13:00 h, with similar maximum values at around 12:00 h. A decrease in $NEP_{SHARQ}$ in the late

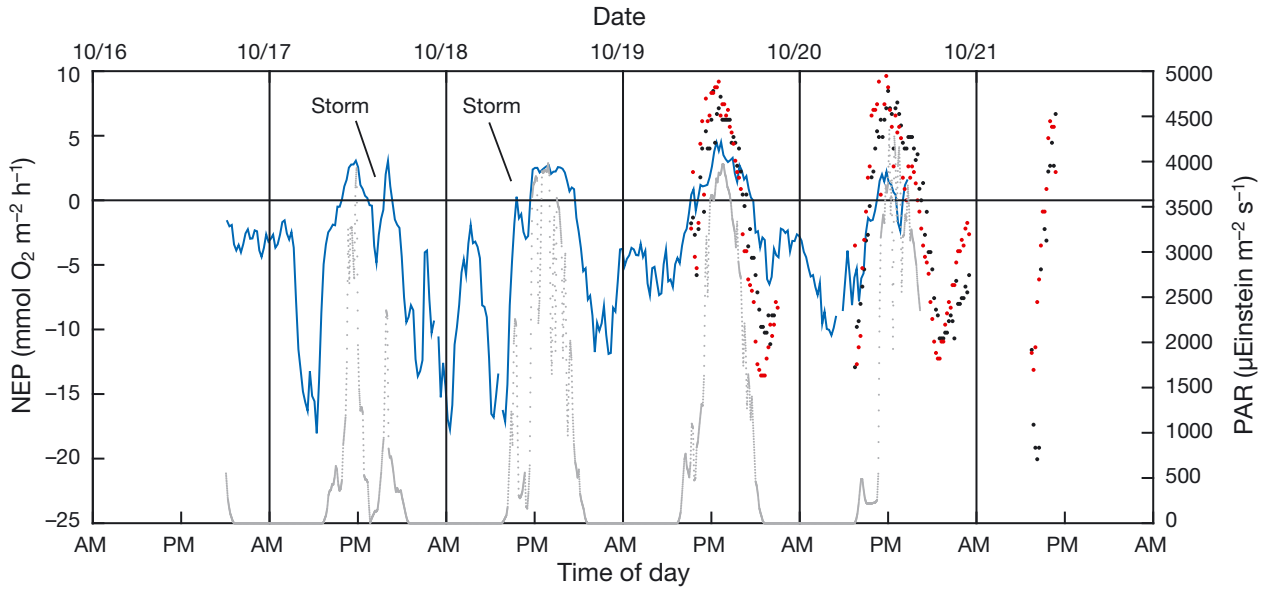


Fig. 6. $NEP_{CROSS}$ 20 min bin average (blue line), $NEP_{SHARQ}$ (mmol $O_2$ $m^{-2}$ $h^{-1}$; Chamber 1: red dots, Chamber 2: black dots) and PAR above the surface (µEinstein $m^{-2}$ $s^{-1}$, grey dots) at the coral reef site from October 16 to 21, 2012

morning of October 17 coincided with a decrease in PAR. At night, $NEP_{SHARQ}$ was relatively constant at a negative value of −6.2 ± 1.0 mmol $O_2$ $m^{-2}$ $h^{-1}$ (Fig. 3).

At the coral reef site, positive $NEP_{SHARQ}$ was observed between 07:30 and 18:00 h. The average maxima from the 2 chambers at around 12:00 h were 8.6 ± 1.0 mmol $O_2$ $m^{-2}$ $h^{-1}$ and lower than those for the seagrass site, even when average PAR values at the coral reef site (800 µEinstein $m^{-2}$ $s^{-1}$; Fig. 5a) were relatively higher. Immediately after dusk (19:30 h), the coral reef site reached negative NEP, with minimum values of −12.5 ± 1.0 mmol $O_2$ $m^{-2}$ $h^{-1}$. $NEP_{SHARQ}$ increased (i.e. was less negative) during early hours of the night (from 20:00 to 23:00 h) on October 20. For the rest of the night (from 20:00 h on October 19 to 07:00 h on October 20 and from 23:00 h on October 20 to 07:00 h on October 21) SHARQ operations were postponed to allow for venting of low $O_2$ water from the enclosures.

$NEP_{CROSS}$ at the coral reef site showed similar diurnal variation as $NEP_{SHARQ}$ (number of observations = 133); linear regression $NEP_{CROSS}$ vs. $NEP_{SHARQ}$: adj. $R^2 = 0.68$, $p < 0.0001$). Positive daily values (20 min bin average) during SHARQ deployment on October 19 and 20 reached 4.5 ± 2.4 mmol $O_2$ $m^{-2}$ $h^{-1}$ and negative values of −11.8 ± 6.0 mmol $O_2$ $m^{-2}$ $h^{-1}$ (Fig. 6). Smaller decreases in net respiration (or increase in NEP) were observed during the night. During a few hours during the nights of October 17 and 18, $NEP_{CROSS}$ was lower (−18.0 mmol $O_2$ $m^{-2}$ $h^{-1}$), possibly due to higher current speeds affecting the $O_2$ gradient; such currents do not affect the community contained within the SHARQ enclosure. Similarly, as observed by SHARQ at the seagrass site, a decrease in $NEP_{CROSS}$ was observed starting in the late morning of October 17, coinciding with the decrease in solar radiation associated with a thunderstorm. A decrease in $NEP_{CROSS}$ was also detected during another storm on October 18.

### Net ecosystem calcification ($NEC_{SHARQ}$)

$NEC_{SHARQ}$ showed diurnal variability with values ranging from −0.15 ± 0.04 to 0.20 ± 0.04 g $CaCO_3$ $m^{-2}$ $h^{-1}$ at the seagrass site, and −0.10 ± 0.04 to 0.17 ± 0.04 g $CaCO_3$ $m^{-2}$ $h^{-1}$ at the coral reef site (Fig. 5b). During daylight hours, NEC was mostly positive at both sites. At night, NEC was negative. TA from discrete measurements at both sites taken inside the 2 SHARQ chambers (Fig. 3b, red and black) and in the ambient water adjacent to the chambers (Fig. 3b, blue) showed TA minimum values at around dusk, and increasing values at night.

These NEC and TA patterns suggest that conditions are favorable for net carbonate dissolution at night. However, our limited data suggest that the balance in NEC over 24 h periods was most likely positive at both sites during the absence of storms. NEC at both sites was positively correlated with NEP (Fig. 7). At the time of maximum daily irradiance, similar NEC (mmol $CaCO_3$ $m^{-2}$ $h^{-1}$):NEP (mmol $O_2$ $m^{-2}$ $h^{-1}$) ratios were observed at the seagrass site (0.2) and the coral reef site (0.3). Average PQ values over

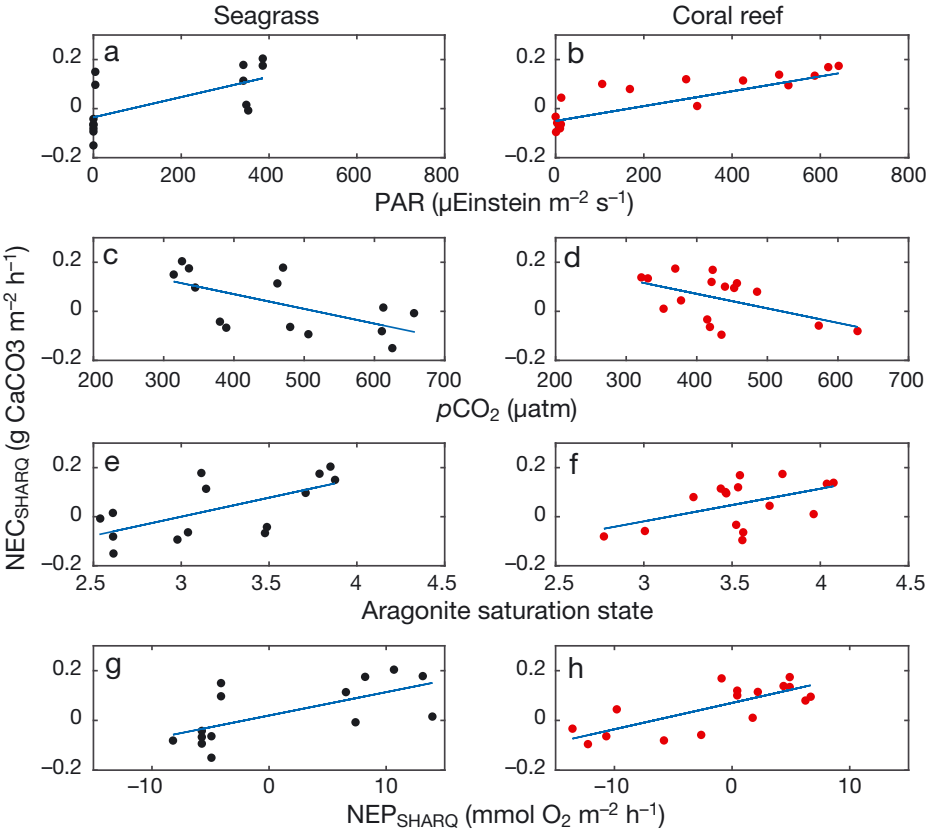


Fig. 7. (a,b) Net community calcification (NEC$_{SHARQ}$; g $CaCO_3$ m$^{-2}$ h$^{-1}$) vs. photosynthetically active radiation (PAR; µEinstein m$^{-2}$ s$^{-1}$), (c,d) NEC$_{SHARQ}$ vs. partial pressure of carbon dioxide ($pCO_2$; µatm), (e,f) NEC$_{SHARQ}$ vs. aragonite saturation state ($\Omega_{ar}$) and (f,g) NEC$_{SHARQ}$ vs. net community production (NEP$_{SHARQ}$; mmol $O_2$ m$^{-2}$ h$^{-1}$) at the seagrass (left) and coral reef (right) sites. Blue line represents linear regression

4 h time intervals from 07:00 to 11:00 h (morning), 11:00 to 15:00 h (mid-day), and 15:00 to 19:00 h (afternoon/evening) were 0.5, 0.9, and 2.6 at the seagrass site, and 1.1, 1.2, and 1.4 at the coral reef site.

### $\Omega_{ar}$, $pCO_2$, and NEP threshold and the compensation light intensities

Replicate NEC$_{SHARQ}$ (Chambers 1 and 2) vs. $\Omega_{ar}$, $pCO_2$, NEP $_{SHARQ}$, and PAR are presented for both seagrass and coral reef sites in Fig. 7. The results from univariate linear regressions are presented in Table 2. 'Threshold values' are defined as zero intercepts (NEC$_{SHARQ}$ = 0), and slopes of the regression lines represent sensitivity of NEC to the given variable. We found slightly lower $\Omega_{ar}$ and NEP thresholds, and lower compensation light intensity at the seagrass site than at the coral reef site, while the $pCO_2$ threshold was slightly higher. The response (slope) of NEC to $\Omega_{ar}$ was stronger in seagrass. At the seagrass site, all the regressions were fairly significant and at similar levels to one another (see p-values in Table 2). At the coral reef site, the NEC vs. PAR regression was highly significant, as was NEC vs. NEP. Relationships of NEC with $pCO_2$ and $\Omega_{ar}$, were moderately and marginally significant, respectively.

Table 2. Univariate linear regression parameters for net community calcification (NEC) vs. aragonite saturation state ($\Omega_{ar}$), partial pressure of carbon dioxide ($pCO_2$), net community production (NEP) and photosynthetically active radiation (PAR) using discrete carbonate parameters measured at 3.6 m depth at the seagrass (16 and 17 October 2012; n = 14) and at 5 m depth at the coral reef site (19 to 21 October 2012; n = 16) within Submersible Habitat for Analyzing Reef Quality (SHARQ) chambers, and PAR at the seafloor outside the chambers. Slope, intercept and threshold data are means ± SE

| | Slope (×10$^{-2}$) | Intercept (×10$^{-2}$) | Adj. $R^2$ | p | Threshold (NEC = 0) |
|---|---|---|---|---|---|
| **Seagrass** | | | | | |
| $\Omega_{ar}$ | 15.47 ± 5.29 | −46.5 ± 17.1 | 0.37 | 0.0128 | 3.1 ± 0.1 |
| $pCO_2$ | −0.06 ± 0.02 | 30.9 ± 10.7 | 0.33 | 0.0194 | 485 ± 28 |
| NEP | 0.94 ± 0.32 | 1.9 ± 2.6 | 0.37 | 0.0123 | −0.2 ± 1.8 |
| PAR | 0.04 ± 0.01 | −3.3 ± 3.3 | 0.36 | 0.0131 | 124 ± 41 |
| **Coral reef** | | | | | |
| $\Omega_{ar}$ | 13.28 ± 6.34 | −41.8 ± 22.6 | 0.18 | 0.0548 | 3.4 ± 0.1 |
| $pCO_2$ | −0.06 ± 0.03 | 30.8 ± 11.6 | 0.21 | 0.0414 | 455 ± 21 |
| NEP | 1.02 ± 0.24 | 6.8 ± 1.6 | 0.53 | 0.0008 | −4.4 ± 1.4 |
| PAR | 0.03 ± 0.01 | −2.9 ± 1.9 | 0.70 | <0.0001 | 142 ± 40 |

Multiple regression of NEC against all 4 explanatory variables ($\Omega_{ar}$, $pCO_2$, $NEP_{SHARQ}$, and PAR) showed that the overall regression at the seagrass site was highly significant (p = 0.0008) and could explain 86% of variability in NEC. However, the individual regressors were not highly significant, which is likely due to multicollinearity with 2 strong correlations amongst the explanatory variables; $pCO_2$ and $\Omega_{ar}$ (–0.99) and PAR and NEP (0.96). This suggests only 2 of 4 explanatory variables may be needed. All regression variable selection procedures suggested that NEC at the seagrass site was best explained with NEP and $\Omega_{ar}$ (85.5%); however, PAR and $pCO_2$ provide reasonably good predictive relations (83%) and can be more easily measured. At the coral reef site, the overall multiple regression model was also highly significant ($p < 10^{-5}$). This model could explain 92% of variability in NEC. The forward selection algorithm chooses PAR as the most important explanatory parameter, which alone could explain 72% of variability in NEC. This is consistent with the univariate regressions. The other variable selection procedures suggest that the full model (corresponding to the multiple regression above with all variables) was the most appropriate model to explain variability in NEC. This interaction model suggests that the response of NEC to $pCO_2$ and $\Omega_{ar}$ variables depends on being in coral reef or seagrass, while the response to NEP and PAR was not significantly different between habitats.

The compensation light intensity for NEC using univariate linear regression of $NEC_{SHARQ}$ vs. PAR data (Fig. 7) shows that $NEC_{SHARQ}$ = 0 at 124 ± 41 µEinstein m$^{-2}$ s$^{-1}$ at the seagrass site, and 142 ± 40 µEinstein m$^{-2}$ s$^{-1}$ at the coral reef site (Table 2). Although there were no $NEC_{SHARQ}$ measurements available at the seagrass site for PAR between 0 to 300 µEinstein m$^{-2}$ s$^{-1}$, the regression indicates that NEC will decrease with a decrease in PAR. $NEP_{SHARQ}$ vs. PAR at the seafloor outside the chambers for seagrass and coral reef is presented in Fig. 8. The compensation light intensities for NEP calculated using Eq. (5) at the seagrass site and coral reef site were 100 ± 9 and 227 ± 31 µEinstein m$^{-2}$ s$^{-1}$, respectively. The values of all fitted parameters are given in Table 3.

## DISCUSSION

Our values of $NEP_{SHARQ}$ at the coral reef site (–12.5 ± 1.0 to 8.6 ± 1.0 mmol $O_2$ m$^{-2}$ h$^{-1}$) were within the range of those observed by previous studies. McGillis et al. (2011) reported coral production of –12.3 to

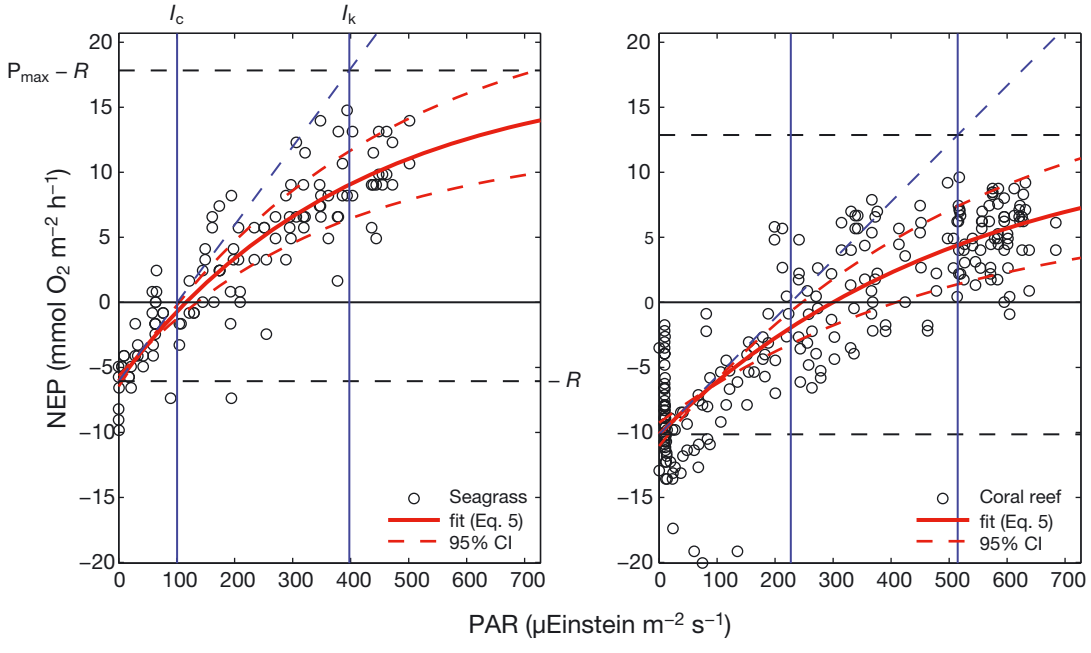


Fig. 8. $NEP_{SHARQ}$ (mmol $O_2$ m$^{-2}$ h$^{-1}$) from Chamber 1 and Chamber 2 vs. PAR (µEinstein m$^{-2}$ s$^{-1}$) at the seafloor outside the chambers for seagrass (left panel) and coral reef (right panel) habitats. Eq. (5) was used to fit the data (solid and dashed red lines). Fitted parameters $NEP_{max}$ (i.e. $P_{max} - R$) and $R$ are shown with the upper and lower, black dashed horizontal lines, respectively. The dashed blue line is NEP = $\alpha \cdot$ PAR – $R$. The vertical blue lines indicate the compensation irradiance ($I_c$) and the saturation irradiance ($I_k$), from left to right, respectively. See Fig. 5 and Table 3 for definitions

Table 3. $NEP_{SHARQ}$ vs. PAR fitted parameters using Eq. (5). $P_{max}$ (mmol $O_2$ $m^{-2}$ $h^{-1}$) is maximum photosynthetic rate, α (mmol $O_2$ $m^{-2}$ $h^{-1}$ [µEinstein $m^{-2}$ $s^{-1}$]$^{-1}$) is the initial slope at low PAR, $R$ is respiration rate (mmol $O_2$ $m^{-2}$ $h^{-1}$), $NEP_{max}$ = $P_{max}$ – $R$ (mmol $O_2$ $m^{-2}$ $h^{-1}$) and $I_c$ and $I_k$ are the compensation and the saturation irradiances (µEinstein $m^{-2}$ $s^{-1}$). All values are means ± SD

| Parameter | Seagrass | Coral reef |
|---|---|---|
| $P_{max}$ | 23.9 ± 2.9 | 23.0 ± 3.3 |
| α | 6.01 ± 0.50 (×$10^{-2}$) | 4.47 ± 0.58 (×$10^{-2}$) |
| $R$ | 6.1 ± 0.2 | 10.2 ± 0.5 |
| $NEP_{max}$ | 17.8 ± 3.0 | 12.9 ± 3.3 |
| $I_c$ | 100 ± 9 | 227 ± 31 |
| $I_k$ | 398 ± 60 | 515 ± 99 |

13.7 mmol $O_2$ $m^{-2}$ $h^{-1}$ estimated by CROSS, and –11.0 to 12.9 mmol $O_2$ $m^{-2}$ $h^{-1}$ from SHARQ observations at Cayo Enrique Reef, Puerto Rico. Rogers (1979) measured NEP as high as 13 mmol $O_2$ $m^{-2}$ $h^{-1}$ at San Cristobal reef, Puerto Rico using a flow-through enclosure, while Falter et al. (2008) reported –8.3 to 7.9 mmol $O_2$ $m^{-2}$ $h^{-1}$ at the Kaneohe Bay Barrier Reef, Hawaii, using Eulerian methods. In the present study, highest net respiration in the coral reef habitat occurred immediately after dusk. A decrease in net respiration in the early hours of the night was consistent with many other studies that show variable rates of respiration during dark hours (Falter et al. 2011, Long et al. 2013, Smith et al. 2013).

The seagrass $NEP_{SHARQ}$ (–6.2 ± 1.0 to 12.3 ± 1.0 mmol $O_2$ $m^{-2}$ $h^{-1}$) was also in the range of values reported by Duarte et al. (2010), derived from a total of 155 different sites around the world. Furthermore, Naumann et al. (2013) report mean NEP of 8 ± 7 mmol $O_2$ specimen area $m^{-2}$ $d^{-1}$ in the Caribbean Reef Lagoon in Puerto Morelos, Mexico. Comparing rates across various studies is difficult, since many studies do not report values normalized to surface area. Higher resolution quantification of our seagrass site in terms of shoot density, biomass and percent coverage for the seagrass would allow for better comparison. Our observations suggest that at both the seagrass and coral reef sites, NEP balance over the 24 h period was slightly negative.

Our NEC estimates at the coral reef site (–35 ± 0.4 to 50 ± 0.4 mmol $CaCO_3$ $m^{-2}$ $d^{-1}$) were on the lower end of a broad range of NEC estimated based upon community metabolism, from –22 to 331 mmol $CaCO_3$ $m^{-2}$ $d^{-1}$ (Langdon & Atkinson 2005, Yates & Halley 2006, Silverman et al. 2007, Bates et al. 2010, Shamberger et al. 2011, Falter et al. 2012, Albright et al. 2013, Foster et al. 2014). NEC values at the seagrass site were remarkably similar to NEC at the coral reef site despite the significant differences in community. The $NEC_{SHARQ}$:$NEP_{SHARQ}$ ratio was also within the wide range of values (0.14 to 12.1) reported by Yates et al. (2014) that represent different reef environments, experimental settings, seawater physical-chemical conditions, and temporal and spatial scales.

The $\Omega_{ar}$ and $pCO_2$ 'critical threshold values' (3.4 ± 0.1 and 455 ± 21 µatm) and the sensitivity of $NEC_{SHARQ}$ to changes in $\Omega_{ar}$ and $pCO_2$ based on univariate linear regression at the coral reef were within a broad range of values reported previously in coral reef ecosystems and coral mesocosms (Langdon et al. 2003, Yates & Halley 2006, Silverman et al. 2007, Andersson et al. 2009, Shamberger et al. 2011). These studies suggested that the NEC threshold of a given coral reef is dependent in large part on live coral cover. A system with higher coral cover could exhibit net calcification at $pCO_2$ (or saturation state) levels lower than those of a system with reduced coral cover. NEC showed an increasing trend with PAR, consistent with previous studies of coral reefs (Langdon & Atkinson 2005, Albright et al. 2013); however, our slope of $NEC_{SHARQ}$ vs. PAR was lower. This may be due to lower PAR during our observations than in Langdon & Atkinson (2005) and Albright et al. (2013), and different community composition. At the seagrass site, we found slightly lower $\Omega_{ar}$ and NEP thresholds and compensation light intensity for NEC compared to the coral reef site, while the $pCO_2$ threshold was slightly higher. This observation suggests that elevated NEP (or $NEP_{max}$) in seagrass beds could allow for higher $pCO_2$ thresholds and lower $\Omega_{ar}$ thresholds for NEC. For example, it is possible that, when the saturation state threshold is crossed, NEC might remain positive under elevated NEP.

The full regression model corresponding to the multiple regression of NEC with all 4 environmental variables ($\Omega_{ar}$, $pCO_2$, NEP and PAR) explained the highest percent of the variability in NEC at both sites. At the coral reef site, PAR alone was a key explanatory variable for NEC, suggesting that NEC at our coral reef could be reasonably well predicted from PAR alone. At the seagrass site, NEC was best explained with 2 variables, NEP and $\Omega_a$; however, PAR and $pCO_2$ provided reasonably good predictive relations and can be more easily measured. The lower correlation of NEC with PAR at the seagrass site may be due to the lack of data between 100 and 300 µEinstein $m^{-2}$ $s^{-1}$ or modification of the light field in the seagrass canopy.

Our value of compensation light intensity ($I_c$) for NEP at the coral reef site (227 ± 31 µEinstein $m^{-2}$ $s^{-1}$)

(Fig. 8) falls between values observed by Long et al. (2013) of 300 µEinstein $m^{-2}$ $s^{-1}$ in coral reefs at the Florida Keys, Albright et al. (2013) of approx. 150 µEinstein $m^{-2}$ $s^{-1}$ in the central Great Barrier Reef and Langdon & Atkinson (2005) of 80 ± 33 µEinstein $m^{-2}$ $s^{-1}$ in an experimental flume. Our light-saturation value ($I_k$) of 515 ± 99 µEinstein $m^{-2}$ $s^{-1}$ (Fig. 8) is similar to values (586 ± 108 µEinstein $m^{-2}$ $s^{-1}$) reported by Langdon & Atkinson (2005), while our slope of the curve (α) is slightly lower (0.06 ± 0.05 vs. 0.13 ± 0.03). At the seagrass site, we observed higher $I_c$ (100 ± 9 µEinstein $m^{-2}$ $s^{-1}$) than the range of 9 to 55 µEinstein $m^{-2}$ $s^{-1}$ previously reported by Pollard & Greenway (2013) in Cairns Harbour, Queensland, on the tropical east coast of Australia. The compensation light intensity likely varies, however, with season and environmental conditions (temperature, nutrients, seawater chemistry). Hourly and daily rates of respiration can follow light-driven changes in production, such that the compensation is driven more by the balance between the supply and demand of fixed carbon and nutrient history (Falter et al. 2011). Higher initial slope of the curve (α) and higher $NEP_{max}$ were observed at the seagrass site than at the coral reef site. This suggests that seagrass (1) exhibits a faster rate change to increased light intensities at lower irradiance, (2) has a higher photosynthetic efficiency, and (3) reaches higher NEP at stronger light levels. These parameters are species-specific, and are influenced by a variety of factors, such as nutrient concentration, temperature and the physiological capabilities. Seagrass also showed lower $I_c$ values for both NEP and NEC than the coral reef site. However, the difference in values between the sites is larger for NEP than for NEC, and this may be a consequence of the lack of measurements available at the seagrass site for PAR between 0 and 300 µEinstein $m^{-2}$ $s^{-1}$, or different responses of 2 metabolic processes to light. Our observations suggest that seagrass is more resistant to periods of low ambient light level conditions. This could be beneficial for these coastal benthic habitats under conditions of increased water turbidity during storms, increased river flows, and increases in agricultural and urban/industrial runoff.

Our CROSS data at the coral reef site showed $O_2$ values (110–195 µM) slightly lower than that reported by McGillis et al. (2011) (180–250 µM) at Cayo Enrique Reef, Puerto Rico, and within the range of values of 100 to 300 µM at the Kaneohe Bay Barrier Reef, Hawaii (Falter et al. 2008). We found relatively low pH variability (7.87–7.99) over our short observation interval in comparison to previous observations at coral reefs (Kayanne et al. 2005 [7.9–8.4]; Yates & Halley 2006 [7.82–8.42]; Manzello 2010 [7.65–8.26]; Santos et al. 2011 [7.7–8.4]; Gray et al. 2012 [7.89–8.17]). This may be a result of local species composition, nutrient availability, tidal flushing and circulation or water depth. For example, Price et al. (2012) showed that deeper reef sites experienced significantly less variability in daily pH than shallow reef habitats.

We observed a strong correlation between pH, $O_2$ and ambient light levels, indicating that, during the day, primary production was a dominant process controlling the diurnal cycles of $O_2$ and pH (Kleypas et al. 2011). During the night, our data showed unexpected small increases in $O_2$ (25 µM), pH (0.02 units), and TA (30 µmol $kg^{-1}$). These small increases are likely a consequence of the advection of different water masses due to tidal or other water movement. Due to the short duration of this field program, the daylight and tidal cycles were largely in the same relative phase. Collecting a longer series of observations would result in cases in which photosynthetic and tidal cycles were also out of phase. This would allow an assessment of the relative contribution of *in situ* production/consumption of oxygen and tidally driven transport to the observed oxygen and pH dynamics and provide more reliable estimates of long-term net production and net calcification.

Although our observations were of short duration and included only 3 thunderstorms, both SHARQ and CROSS data showed that thunderstorms temporarily influence NEP in both seagrass and coral reef environments. A decrease of ambient light significantly lowered NEP and changed the system from a positive net production to one in which respiration dominated. This is consistent with previous reports (Falter et al. 2011, Naumann et al. 2013). The decrease in NEC with decrease in PAR implies that daytime tropical storms also have an impact on annual NEC estimates. During the night storm, changes in the water column $O_2$ concentration and pH were not caused by benthic community metabolism (NEP and NEC) responses to ambient light; therefore, these changes were likely related to advection/mixing. We observed slight decreases in oxygen concentration at the upper optodes and increases in oxygen concentration and pH at the lower optodes. This pattern is consistent with enhanced mixing during storms that causes the upper and lower oxygen concentrations to converge toward similar values. Similar increases in oxygen and pH were also observed in the night without a storm and could be caused by tides/advection. Since the water column oxygen was slightly undersaturated with respect to the atmosphere, gas ex-

change could cause an increase of oxygen in the upper water column. However, this is not consistent with the decrease in oxygen that was observed. Longer time series are needed to determine whether strong and frequent storms have a significant effect on the long-term balance of production and respiration. Since the frequency and intensity of storms in tropical areas is expected to increase with climate change (Webster et al. 2005), it is important to evaluate their impacts on the NEC caused by attenuation of incident light relative to the impacts due to ocean acidification.

Salinity-normalized values of $TCO_2$ and TA in the SHARQ chambers were slightly lower at the seagrass site than at the coral reef site. Water at the seagrass site, which was close to the shoreline, can be considered an end-member with respect to water moving across the reef system from the shoreline to the open ocean. $TCO_2$ and TA could be depleted at this seagrass end member due to uptake of $TCO_2$ and TA by photosynthesis and calcification that occurs across both the seagrass and coral reef habitats. Our average values of $TCO_2$, $TCO_{2n}$, TA, and $TA_n$ at both sites were slightly lower than values observed at nearby locations in the Lower Keys during autumn 2010 and 2011 by Manzello et al. (2012) (Table 1), but fall within the range of their yearly values. Manzello et al. (2012) sampled carbon chemistry at an inshore seagrass dominated location (24.59723 °N, 81.45505 °W) and an offshore (24.55141° N, 81.40251 °W) coral reef site. They reported higher values of $TCO_2$, $TCO_{2n}$, TA, and $TA_n$ at the inshore seagrass site in comparison to the offshore coral reef site during autumn, but this pattern reversed going into spring and summer. Such differences would depend on multiple factors including biomass, seagrass species, ambient light, water residence time (tidal flushing), and water depth.

During our short observation time frame, we did not observe significant increases in pH and $\Omega_{ar}$ values at the seagrass site relative to the adjacent coral reef site as observed in previous studies (Unsworth et al. 2012, Buapet et al. 2013). On the contrary, pH and $\Omega_{ar}$ at the seagrass site were slightly lower. A number of factors could have contributed to this observation including: (1) a short period of optimal light ($I_c$ > 100 µEinstein $m^{-2}$ $s^{-1}$) for NEP and thus repressed production in seagrass beds, (2) differences in residence times between the coral reef and the seagrass bed which may have resulted in different levels of mixing with the surrounding waters, and (3) elevation of $CO_2$ due to calcification and respiration of non-photosynthetic organisms (like shellfish) living in the seagrass beds.

Simultaneous SHARQ deployments at both sites would allow for more rigorous comparison of community metabolism between sites. The ability to differentiate the contribution of mass transport processes (e.g. advection) to oxygen and carbon dynamics in the system, from reaction processes (production, respiration, calcification, dissolution) would be improved by additional physical measurements, including linear arrays of stations perpendicular to the shoreline or orthogonal arrays. The short duration of our deployments made it difficult to make definitive statements regarding the long-term balance in the organic or inorganic ($CaCO_3$) carbon budgets. Such measurements would need to be performed seasonally, at a resolution of at least weekly and under a range of environmental conditions, to evaluate annual net production and/or calcification of different seagrass and coral reef communities and their variability.

*Acknowledgements*. This work was possible through collaboration between the University of South Florida, the U.S. Geological Survey (USGS), the Florida Fish and Wildlife Conservation Commission, Dalhousie University, Columbia University, NOAA, NASA, and the Institute of Marine Affairs in Trinidad and Tobago. Field work was supported by NASA grant NNH10ZDA001NRA-UAS ('High Resolution Assessment of Carbon Dynamics in Seagrass and Coral Reef Biomes') funded by NASA's Airborne Science program for UAS Enabled Earth Science Program, and by the Coastal and Marine Geology Program of the U.S. Geological Survey. We thank research technician Nathan Smiley and dive safety officer, Marc Blouin, from the USGS, and Captain Joe Bailey, and staff of the dive boat 'Playmate'. D.T. and C.L'E. were funded by the Canada Excellence Research Chair (CERC) in Ocean Science and Technology. This is LDEO contribution 7909. References to non-USGS products and services are provided for information only, and do not constitute endorsement or warranty, expressed or implied, by the U.S. Government, as to their suitability, content, usefulness, functioning, completeness, or accuracy.

## LITERATURE CITED

Albright R, Langdon C, Anthony KRN (2013) Dynamics of seawater carbonate chemistry, production, and calcification of a coral reef flat, central Great Barrier Reef. Biogeosciences 10:6747–6758

Andersson AJ, Gledhill D (2013) Ocean acidification and coral reefs: effects on breakdown, dissolution, and net ecosystem calcification. Ann Rev Mar Sci 5:321–348

Andersson AJ, Kuffner IB, Mackenzie FT, Jokiel PL, Rodgers KS, Tan A (2009) Net loss of $CaCO_3$ from a subtropical calcifying community due to seawater acidification: mesocosm-scale experimental evidence. Biogeosciences 6:1811–1823

Anthony KRN, Kleypas JA, Gattuso JP (2011) Coral reefs modify their seawater carbon chemistry — implications for impacts of ocean acidification. Glob Change Biol 17: 3655–3666

Bates NR, Amat A, Andersson AJ (2010) Feedbacks and responses of coral calcification on the Bermuda reef system to seasonal changes in biological processes and ocean acidification. Biogeosciences 7:2509–2530

Brock JC, Yates KK, Halley RB (2006a) Integration of coral reef ecosystem process studies and remote sensing. In: Richardson LL, LeDrew EF (eds) Remote sensing of aquatic coastal ecosystem processes: science and management applications. Springer, Dordrecht, p 111–131

Brock JC, Yates KK, Halley RB, Kuffner IB, Wright CW, Hatcher BG (2006b) Northern Florida reef tract benthic metabolism scaled by remote sensing. Mar Ecol Prog Ser 312:123–139

Buapet P, Gullström M, Björk M (2013) Photosynthetic activity of seagrasses and macroalgae in temperate shallow waters can alter seawater pH and total inorganic carbon content at the scale of a coastal embayment. Mar Freshw Res 64:1040–1048

Dickson AG (1990) Standard potential of the reaction: $AgCl(s)+1/2H_2(g) = Ag(s)+HCl(aq)$, and the standard acidity constant of the ion $HSO_4$ in synthetic sea water from 273.15 to 318.15 K. J Chem Thermodyn 22:113–127

Dickson A, Millero FJ (1987) A comparison of the equilibrium constants for the dissociation of carbonic acid in seawater media. Deep-Sea Res 34:1733–1743

Dickson AG, Sabine CL, Christian JR (eds) (2007) Guide to best practices for ocean $CO_2$ measurements. PICES special publication 3. http://cdiac.ornl.gov/ftp/oceans/Handbook_2007/Guide_all_in_one.pdf

Doney SC, Fabry VJ, Feely RA, Kleypas JA (2009) Ocean acidification: the other $CO_2$ problem. Ann Rev Mar Sci 1: 169–192

Duarte CM, Marbà N, Gacia E, Fourqurean JW, Beggins J, Barron C, Apostolaki ET (2010) Seagrass community metabolism: assessing the carbon sink capacity of seagrass meadows. Global Biogeochem Cycles 24:GB4032, doi:10.1029/2010GB003793

Fabricius KE, Langdon C, Uthicke S, Humphrey C and others (2011) Losers and winners in coral reefs acclimatized to elevated carbon dioxide concentrations. Nat Clim Change 1:165–169

Falter JL, Lowe RJ, Atkinson MJ, Monismith SG, Schar DW (2008) Continuous measurements of net production over a shallow reef community using a modified Eulerian approach. J Geophys Res 113:C07035, doi:10.1029/2007JC004663

Falter JL, Atkinson MJ, Schar DW, Lowe RJ, Monismith SG (2011) Short-term coherency between gross primary production and community respiration in an algal-dominated reef flat. Coral Reefs 30:53–58

Falter JL, Lowe RJ, Atkinson MJ, Cuet P (2012) Seasonal coupling and decoupling of net calcification rates from coral reef metabolism and carbonate chemistry at Ningaloo Reef, Western Australia. J Geophys Res 117:C05003, doi:10.1029/2011JC007268

Foster T, Short JA, Falter JL, Ross C, McCulloch MT (2014) Reduced calcification in Western Australian corals during anomalously high summer water temperatures. J Exp Mar Biol Ecol 461:133–143

Gattuso JP, Frankignoulle M, Smith SV (1999) Measurement of community metabolism and significance in the coral reef $CO_2$ source-sink debate. Proc Natl Acad Sci USA 96:13017–13022

Gattuso JP, Kirkwood W, Barry JP, Cox E and others (2014) Free ocean $CO_2$ enrichment (FOCE) systems: present status and future developments. Biogeosci Disc 11: 4001–4046

Gray SEC, DeGrandpre MD, Langdon C, Corredor JE (2012) Short-term and seasonal pH, $pCO_2$ and saturation state variability in a coral-reef ecosystem. Global Biogeochem Cycles 26:GB3012, doi:10.1029/2011GB004114

Hatcher BG (1997) Organic production and decomposition. In: Birkeland C (ed) Life and death of coral reefs. Chapman and Hall, New York, NY, p 140–174

Invers O, Romeo J, Perez M (1997) Effects of pH on seagrass photosynthesis: a laboratory and field assessment. Aquat Bot 59:185–194

Jury CP, Whitehead RF, Szmant AM (2010) Effects of variations in carbonate chemistry on the calcification rates of *Madracis auretenra* (=*Madracis mirabilis* sensu Wells, 1973): bicarbonate concentrations best predict calcification rates. Glob Change Biol 16:1632–1644

Kayanne H, Hata H, Kudo S, Yamano H and others (2005) Seasonal and bleaching-induced changes in coral reef metabolism and $CO_2$ flux. Global Biogeochem Cycles 19: GB3015, doi:10.1029/2004GB002400

Kleypas JA, Yates KK (2009) Coral reefs and ocean acidification. Oceanography (Wash DC) 22:108–117

Kleypas JA, Anthony KRN, Gattuso JP (2011) Coral reefs modify their seawater carbon chemistry—case study from a barrier reef (Moorea, French Polynesia). Glob Change Biol 17:3667–3678

Kline DI, Teneva L, Schneider K, Miard T and others (2012) A short-term *in situ* $CO_2$ enrichment experiment on Heron Island (GBR). Sci Rep 2:413

Langdon C, Atkinson MJ (2005) Effect of elevated $pCO_2$ on photosynthesis and calcification of corals and interactions with seasonal change in temperature/irradiance and nutrient enrichment. J Geophys Res 110:1–16

Langdon C, Takahashi T, Sweeney C, Chipman D and others (2000) Effect of calcium carbonate saturation state on the calcification rate of an experimental coral reef. Global Biogeochem Cycles 14:639–654

Langdon C, Broecker WS, Hammond DE, Glenn E and others (2003) Effect of elevated $CO_2$ on the community metabolism of an experimental coral reef. Global Biogeochem Cycles 17:1011, doi:10.1029/2002GB001941

Lawrence D, Dagg MJ, Liu HB, Cummings SR, Ortner PB, Kelble C (2004) Wind events and benthic–pelagic coupling in a shallow subtropical bay in Florida. Mar Ecol Prog Ser 266:1–13

Liu X, Patsavas MC, Byrne RH (2011) Purification and characterization of meta-cresol purple for spectrophotometric seawater pH measurements. Environ Sci Technol 45: 4862–4868

Long MH, Berg P, de Beer D, Zieman JC (2013) In situ coral reef oxygen metabolism: an eddy correlation study. PLoS ONE 8:e58581

Manzello DP (2010) Ocean acidification hotspots: Spatiotemporal dynamics of the seawater $CO_2$ system of eastern Pacific coral reefs. Limnol Oceanogr 55:239–248

Manzello DP, Enochs IC, Melo N, Gledhill DK, Johns EM (2012) Ocean acidification refugia of the Florida reef tract. PLoS ONE 7:e41715

Marbà N, Holmer M, Gacia E, Barron C (2006) Seagrass bed sand coastal biogeochemistry. In: Larkum AWD, Orth RJ, Duarte CM (eds) Seagrasses: biology, ecology and conservation. Springer, Dordrecht, p 135–157

Marsh JA Jr, Smith SV (1978) Productivity measurements of coral reefs in flowing waters. In: Stoddart DR, Johannes

RE (eds) Coral reefs: research methods. Monographs on oceanographic methodology 5, UNESCO, Paris, p 361–377

McGillis WR, Langdon C, Loose B, Yates KK, Corredor J (2011) Productivity of a coral reef using boundary layer and enclosure methods. Geophys Res Lett 38:L03611, doi:10.1029/2010GL046179

Mehrbach C, Culberson CH, Hawley JE, Pytkowicz RM (1973) Measurement of the apparent dissociation constants of carbonic acid in seawater at atmospheric pressure. Limnol Oceanogr 18:897–907

Moses CS, Andréfouët S, Kranenburg CJ, Muller-Karger FE (2009) Regional estimates of reef carbonate dynamics and productivity using Landsat 7 ETM+, and potential impacts from ocean acidification. Mar Ecol Prog Ser 380: 103–115

Naumann MS, Jantzen C, Haas AF, Iglesias-Prieto R, Wild C (2013) Benthic primary production budget of a Caribbean reef lagoon (Puerto Morelos, Mexico). PLoS ONE 8: e82923

Odum HT, Odum EP (1955) Trophic structure and productivity of a windward coral reef at Eniwetok Atoll, Marshall Islands. Ecol Monogr 25:291–320

Palacios SL, Zimmerman RC (2007) Response of eelgrass *Zostera marina* to $CO_2$ enrichment: possible impacts of climate change and potential for remediation of coastal habitats. Mar Ecol Prog Ser 344:1–13

Pierrot D, Lewis E, Wallace DWR (2006) MS excel program developed for $CO_2$ system calculations. ORNL/CDIAC-105, Tech Rep, Carbon Dioxide Information Analysis Center, Oak Ridge National Laboratory, U.S. Department of Energy, Oak Ridge, TN

Platt T, Gallegos CL, Harrison WG (1980) Photoinhibition of photosynthesis in natural assemblages of marine phytoplankton. J Mar Res 38:687–701

Pollard PC, Greenway M (2013) Seagrasses in tropical Australia, productive and abundant for decades decimated overnight. J Biosci (Bangalore) 38:1–10

Price NN, Martz TR, Brainard RE, Smith JE (2012) Diel variability in seawater pH relates to calcification and benthic community structure on coral reefs. PLoS ONE 7:e43843

Reidenbach MA, Monismith SG, Koseff JR, Yahel G, Genin A (2006) Boundary layer turbulence and flow structure over a fringing coral reef. Limnol Oceanogr 51:1956–1968

Rogers CS (1979) The productivity of San Cristobal Reef, Puerto Rico. Limnol Oceanogr 24:342–349

Santos IR, Glud RN, Maher D, Erler D, Eyre BD (2011) Diel coral reef acidification driven by porewater advection in permeable carbonate sands, Heron Island, Great Barrier Reef. Geophys Res Lett 38:L03604, doi:10.1029/2010GL046053

Seargent MC, Austin TS (1954) Biologic economy of coral reefs. Bikini and nearby atolls, Part 2. Oceanography (biologic). US Geol Surv Prof Pap 260-E:293–300

Semesi IS, Beer S, Björk M (2009) Seagrass photosynthesis controls rates of calcification and photosynthesis of calcareous macroalgae within a seagrass meadow. Mar Ecol Prog Ser 382:41–47

Shamberger KEF, Feely RA, Sabine CL, Atkinson MJ and others (2011) Calcification and organic production on a Hawaiian coral reef. Mar Chem 127:64–75

Silverman J, Lazar B, Erez J (2007) Effect of aragonite saturation, temperature, and nutrients on the community calcification rate of a coral reef. J Geophys Res112:C05004, doi:10.1029/2006JC003770

Silverman J, Lazar B, Cao L, Caldeira K, Erez J (2009) Coral reefs may start dissolving when atmospheric $CO_2$ doubles. Geophys Res Lett 36:L05606, doi:10.1029/2008GL036282

Smith SV (1973) Carbon dioxide dynamics: A record of organic carbon production, respiration, and calcification in the Eniwetok windward reef flat community. Limnol Oceanogr 18:106–120

Smith SV, Key GS (1975) Carbon dioxide and metabolism in marine environments. Limnol Oceanogr 20:493–495

Smith JE, Price NN, Haas A (2013) Coupled changes in dissolved oxygen and pH associated with metabolism of benthic reef organisms. Mar Biol 160:2437–2447

Unsworth RKF, Collier CJ, Henderson GM, McKenzie LJ (2012) Tropical seagrass meadows modify seawater carbon chemistry: implications for coral reefs impacted by ocean acidification. Environ Res Lett 7:024026

Webster PJ, Holland GJ, Curry JA, Chang H-R (2005) Changes in tropical cyclone, number, duration and intensity in a warming environment. Science 309:1844–1846

Wimbush M, Munk W (1970) The benthic boundary layer. In: Maxwell AE (ed) The sea, Vol. 4. John Wiley & Sons, New York, NY, p 731–758

Yao W, Byrne RH (1998) Simplified seawater alkalinity analysis: use of linear array spectrometers. Deep-Sea Res I 45:1383–1392

Yarbro L, Carlson PR Jr, McHan C, Carlson DF and others (2013) Seagrass biomass and productivity in the Florida Keys, USA: ground-level and airborne measurements. American Geophysical Union, fall meeting 2013, abstract #OS33a-1740

Yates KK, Halley RB (2003) Measuring coral reef community metabolism using new benthic chamber technology. Coral Reefs 22:247–255

Yates KK, Halley RB (2006) $CO_2$ concentration and $pCO_2$ thresholds for calcification and dissolution on the Molokai reef flat, Hawaii. Biogeosciences 3:357–369

Yates KK, Dufore C, Smiley N, Jackson C, Halley RB (2007) Diurnal variation of oxygen and carbonate system parameters in Tampa Bay and Florida Bay. Mar Chem 104:110–124

Yates KK, Rogers CS, Herlan JJ, Brooks GR, Smiley NA, Larson RA (2014) Diverse coral communities in mangrove habitats suggest a novel refuge from climate change. Biogeosciences 11:4321–4337

Zhang H, Byrne RH (1996) Spectrophotometric pH measurements of surface seawater at in-situ conditions: absorbance and protonation behavior of thymol blue. Mar Chem 52:17–25

*Editorial responsibility: Steven Lohrenz, New Bedford, Massachusetts, USA*

*Submitted: June 3, 2014; Accepted: June 5, 2015*
*Proofs received from author(s): October 11, 2015*